ICP-MS triple quadrupole as analytical technique to define trace and ultra-trace fingerprint of extra virgin olive oil

ICP-MS Triple Quadrupole as analytical technique to define trace and ultra-trace fingerprint of extra virgin olive oil

Chiara Telloli[1], Silvia Tagliavini[2], Fabrizio Passarini[2], Stefano Salvi[1], Antonietta Rizzo[1]

[1]ENEA, Italian National Agency for New Technologies, Energy and Sustainable Economic Development Fusion and Technology for Nuclear Safety and Security Department Nuclear Safety, Security and Sustainability Division - via Martiri di Monte Sole 4, 40129 Bologna, Italy; chiara.telloli@enea.it; https://orcid.org/0000-0003-1746-6360
[2]Department of Industrial Chemistry "Toso Montanari", University of Bologna, Italy.

*Correspondence: chiara.telloli@enea.it; Tel.: +39 051 6098 485 (office) -109 (lab)

Abstract

Extra virgin olive oil is a typical product of Mediterranean area, and its origin protection is continuously improved. 24 olive oil samples from different geographical origin were analyzed and 40 elements were evaluated with chemometric techniques. This study aims at elaborating a method to determine mineral composition of this matrix and at validating the method used to determine its reliability. The high-level laboratory facilities for trace element/isotopic analysis realized in ENEA Brasimone (Italy) is a useful tool to reduce the limit of detection of elements, cutting down pollutants. Both Clean Laboratory for sample pre-treatment and Clean Room Standard ISO 6 are constantly monitored to guarantee the control quality. The results obtained using ICP-MS Triple Quadrupoles show changes between the analysed samples. Finally, Principal Component Analysis was conducted to better characterize olive oil products from different geographical origin, providing a fingerprint of the element patterns in the samples.

***Keywords**: traceability, extra virgin olive oil, ICP-MS-QQQ, rare earth element.*

1. Introduction

The quality of what we eat has become a real issue highlighting the importance to identify the origin of food commodities for both consumers and producers. European Union Legislation (1992) introduced a discrimination based on Geographical Indicators (European Commission, 2020) testifying the linkage between food and its origin (Council Regulation, 1992). The EU Regulation 178/2002 forced the agro-products traceability requirement.

Unfortunately, it's not always easy to rely on the same parameters for food product's origin determination becouse of variation due to fertilization, type of cultivation, soil composition and geographical origin. On the opposite, trace, and ultra-trace element (REE) could give a useful representative fingerprint of the composition of the product (Aceto et al., 2018).

To do that, analytical technologies involved in this research are numerous, such as optical spectroscopy and mass spectrometry or atomic absorption spectroscopy. Inductive Coupled Plasma Mass Spectrometry (ICP-MS) is one of the most confident and reliable technique for simultaneous multi-element analysis in traceability. Over the last 20 years, different implementations have been developed, as an additional quadrupole has been introduced in front of the Collision/Reaction Cell (CRC) to act as an ulterior mass filter, obtaining the triple quadrupole (ICP-MS-QQQ) technology. ICP-MS-QQQ leads to a better control over the reaction becoming a powerful tool for the interference-free quantitative analysis especially for rare earth elements. Moreover, with two quadrupoles into the instrumentation, also chemical noise is lower allowing a better sensibility and detectability.

It's largely recognized that edible oil, in particularly from Olea Europaea tree, is a characteristic product of the Mediterranean area and a strategic item for its high exportation and consumption. Clearly having a steady growing demand and a high cost of production, Extra Virgin Olive (EVO) oil is much more expensive than other oils and for this reason it may be frequently subjected to adulteration and falsification.

The aim of this study is showing the main mineral composition of EVO oil, which could be apply in a future perspective to illustrate the elements distribution in the matrix. In addition, taking into account different sampling collection areas, the study could be a start to point out significate differences regarding mineral composition, between different origin provenances of EVO oils.

To do this, the use of a triple quadrupole ICP-MS in a Clean Room ISO6 reduces the limit of detection and the limit of quantification of all the elements analysed, and especially the REE elements, which can better discriminate the different kind of EVO oils.

2. Material and methods

2.1. Sample collection

The food characterization through mineral fingerprint determination is based on the analysis of EVO oil samples of different origin. The samples were collected in various parts of Italy with some exception sampling in Albany (as shown in Fig. 1), for a total number of 24 olive oil samples (Table 1) from 2013 to 2018 (Rizzo and Telloli, 2019). All the EVO oil samples come from oil mills, except the EVO oil samples from COOP which are industrial, and the specific origin of the olives is not known, it is only known that they are of Italian origin.

Table 1. List of the sampling site, specifying the location and the respectively province of the EVO oil samples collected and analysed and the year of production.

Sample name	Location	Province
Albany 2014	Albany	-
Albany 2015	Albany	-
Tuscany 2013	Pistoia	Pistoia (PT)
Tuscany 2014	Prato	Prato (PO)
Marche 2015	Colli del Tronto	Ascoli Piceno (AP)
Liguria 2018	Riviera dei Fiori	Imperia (IM)
Abruzzo 2017	Vasto	Chieti (CH)
Calabria 2015a	Crotone	Crotone (CR)
Calabria 2015b	Castrovillari	Cosenza (CS)
Calabria 2015c	Rossano	Cosenza (CS)
Campania 2015	Perdifumo	Salerno (SA)
Campania 2015	Pimonte	Napoli (NA)
Campania 2017	Perdifumo	Salerno (SA)
Sardinia 2016	Ales (OR)	Oristano (OR)
Apulia 2013a	Barletta	Barletta-Andria-Trani (BAT)
Apulia 2013b	Manfredonia	Foggia (FG)
Apulia 2013c	Molfetta	Bari (BA)
Apulia 2014	Molfetta	Bari (BA)
Apulia 2016	Molfetta	Bari (BA)
Apulia 2018a	Manfredonia	Foggia (FG)
Apulia 2018b	Squinzano	Lecce (LE)
Coop FIORE 2013	-	-
Coop FIORE 2014	-	-
Coop Costanza	-	-

2.2. Chemicals

Sample treatment procedures were optimized by reducing all reagent volumes to prevent sample loss and reducing sample manipulation and possible contamination from consumables or atmosphere. For the blank carrier solution and the digestion acid mixture preparation, 69% solution of HNO_3, 37% solution of HCl and ultra-pure grade 30-32% H_2O_2 were acquired from Sigma-Aldrich (St. Louis, MO, USA) and Carlo Erba Reagents (Milan, Italy) respectively. Generally, HNO_3 is used because it favors the oxidation of the almost compounds and minimizes the polyatomic interferences (e.g., Cr, Ni, and As). The high purity deionized water was obtained through Milli-Q® Advantage A10 water purification system (Millipore, Bedford, MA, USA). A multi-element standard stock solution used was the IV-ICP-MS71A (10 µg mL^{-1} each in 3% HNO_3) including 43 elements (Ag, Al, As, B, Ba, Be, Ca, Cd, Ce, Co, Cr, Cs, Cu, Dy, Er, Eu, Fe, Ga, Gd, Ho, K,

La, Lu, Mg, Mn, Na, Nd, Ni, P, Pb, Pr, Rb, S, Se, Sm, Sr, Th, Tl, Tm, U, V, Yb and Zn). For the REEs ultra-trace analysis, the CMS-1 stock Standard solution was selected (10 µg mL^{-1} each in 5% HNO_3) including 18 elements (Ce, Dy, Er, Eu, Gd, Ho, La, Lu, Nd, Pr, Sc, Sm, Tb, Th, Tm, U, Y and Yb). Both standard solutions are produced form Inorganic Ventures (Christiansburg, USA).

2.3. Laboratory facilities

The implementation of high-level laboratory facilities for trace element/isotopic analysis was realized in ENEA C.R. Brasimone (Emilia Romagna region, Italy), where are present both a Clean Laboratory for sample pre-treatment and preparation for ICP-MS analysis and a Clean Room (ISO 14644-1 Clean Room Standard ISO 6 class) with controlled pressure, temperature, and humidity. This clean room satisfies all standard request for food trace analysis, with a maximum concentration limit (particles/m^3) of 1 x 10^6 for particles equal to and larger than 0.1 µm for ISO Class 6.

A Triple quadrupole inductively coupled plasma mass spectrometer (ICP-MS-QQQ) 8800 model (Agilent Technologies, Santa Clara, CA, USA) is located in the clean room. The instrument configuration includes Nickel interface cones, standard ion lens and sample introduction system consisting of a MicroMist glass concentric nebulizer (400 µL min^{-1}), a quartz Scott double-pass spray chamber cooled by a Peltier thermoelectric module down to 2° C to reduce water vapour present in the sample aerosol, and a quartz shielded torch with 2.5 mm injector.

Both the Clean Laboratory and the Clean Room Standard ISO 6 are constantly monitored to guarantee the control quality which reduce the limit of detection of all the elements, cutting down pollutants.

2.4. Sample treatment

The mineralization was carried out with a microwave digestion system, Speedwave Four (Berghof, Germany), equipped with temperature and pressure parameters control. Each EVO oil samples were weighted 400 mg and directly put into TFM^{T}M-PTFE[5] vessels, a perfluorated plastic with perfluoroalkoxy side chain (< 1% by weight). The vessels were then filled with 7 ml of HNO_3 (69%) (Fluka, traceSELECT®) and 1 ml of H_2O_2 (30%) (Carlo Erba) as acid mixture for sample digestion preparation. Each digestion cycle was prepared with four closed vessels, and it was programmed according to the microwave heating program: step 1 with a temperature of 160° C, pressure 40 Bar for 15 min; step 2 with a temperature of 100° C, pressure 40 Bar for 20 min and finally step 3 with a temperature of 50° C, pressure 40 Bar for 10 min. The mineralization acid mixture already reported was tested with different acid solution ratios and the one used was with the lowest amount of acid mixture needful for a clear mineralization. Each sample resulting from the acid digestion was then diluted to 50 ml with the same process solution plus adding 2% of a HNO_3 69% solution and 1% of HCl 37% solution. For the multi-element analysis, EVO oil samples were diluted another time with dilution 1:2 with a final volume of 10 ml. The acid concentration in the final sample was 7.84% HNO_3 and 0.42% HCl. For ultra-trace analysis EVO oil samples, were analysed as they were.

2.5. Validation method parameters

Limit of detection (LOD) and limit of quantification (LOQ) for each element were established for the instrument and the process, according to EURACHEM recommendation. The first ones were calculated starting from the analysis of five instrument blanks with three replicate each. Instrument blank means instrument carrying solution: 2% of HNO_3 and 1% of HCl. To determine its LOD and LOQ standard deviations obtained for each element were multiplied for 3 (3σ) and for 10 (10σ) respectively. The same consideration was done for LOD and LOQ calculation for the process, analysing five process blanks, with three replicate each. The blank of the process refers to the same quantity, 7 mL plus 1 mL of 69 % solution of HNO_3 and 30-32 % solution of H_2O_2 respectively, analysed with ICP-MS-QQQ after a cycle of acid digestion and for each sample mineralized.

Linearity of the external calibration. Two curves of calibration were obtained. One with eight concentrations point in the ppb range: 0.1 ppb, 0.5 ppb, 1 ppb, 5 ppb, 10 ppb, 50 ppb, 100 ppb and 150 ppb, for Be, B, Na, Mg, Al, P, K, Ca, V, Cr, Mn, Fe, Co, Ni, Cu, Zn, Ga, As, Se, Rb, Sr, Ag, Cd, Cs, Ba, Tl, Pb, Th and U. The other for REE in ppt range: 0.1 ppt, 0,25 ppt, 0.5 ppt, 1 ppt, 5 ppt, 10 ppt, 25 ppt and 50 ppt, for La, Ce, Pr, Nd, Sm, Eu, Gd, Tb, Dy, Ho, Er, Tm, Yb and Lu.

Accuracy. According to the purpose of method's validation, a Standard Reference Material (SRM) was used to testify the efficiency of the instrument and to determine systematically a possible bias of the analysis. For EVO oil samples it was not possible having at disposal certified materials with the same or similar matrices, therefore we chose a material

with a prevailing organic matrix: SRM-1573A (Tomato leaves) from NIST. It was weighted 0.0200 g of the Standard Material to be introduced into the vessel for the mineralization. Spiked standard additions consisted in 2 mL of original Standard solution each time, to obtain in the final sample 16 ppb each element for what concerns multi-element trace analysis and 40 ppt for ultra-trace REE analysis. The SRM-1573A sample was digested and prepared as explained in Section 2.3 and analysed with the same approach of the samples. The efficiency of the instrument was verified with the recovery of the analysed material with known concentrations. To cover the elements, absent in the mineral composition of the SRM-1573A spiked standards used for the calibration curves were added to the vessel prior to the digestion cycle to have a complete recovery for each element.

Repeatability and inter-day repeatability. Regarding repeatability, SRM-1573A with spiked standard addition was mineralized and processed by ICP-MS-QQQ five times, with three replicates for each analysis. For inter-day repeatability, three different mineralization of SRM-1573A with spiked standard addition were digested and analysed within three days, keeping three replicates for each analysis.

2.6. Multivariate analysis

Multivariate analysis trough chemometric methods enables the retainment of the useful information minimizing time and costs due to the multiple variables related to the observation of a system. Furthermore, chemometric tools application is required to evaluate the huge number of data resulting from ICP-MS-QQQ analysis, allowing to investigate a possible relationship between the EVO oil samples and their origin of provenance. Principal Component Analysis (PCA) is one of the most important techniques to explore and select data information and has found relevant applications in different sectors, including chemistry, biology, medicine, and economics. PCA works transforming the *original variables* in new variables called *latent variables*, or principal components, obtained from the linear combination of the original variables in order to be orthogonal between each other, representing the orthonormal space's basis. First principal component will represent the maximum variance of the system studied, while the second one, uncorrelated with the first, will represent the maximum residual variance, and so on until covering the total variance of the system. PCA's relevance is mostly due to its capacity to reduce the data dimensionality. In addition, this method eliminates the spurious information, it evaluates each variable's relative relevance, and it allows the visualization of the objects in clusters or in classes, identifying at the same time the presence of outliers. In this study PCA was performed with XLSTAT by Addinsoft program.

3. Results and Discussion

3.1. Validation method parameters for the multi element analysis

Two different operation modes were used: *no gas* and He mode. The second one was used to overcome spectral overlappings due to polyatomic interferences. Interference removal with He in collision mode does not rely on specific reaction pathways, but through the Kinetic Energy Discrimination a decelerating potential is applied excluding low energy ions (polyatomic ions and residual gas ions, the ones that have undergone more collisions with He cell gas).

Isotopes analysed with *no gas* mode were Be, B, Na, Al, P, K, V, Cr, Mn, Fe, Co, Cu, Se, Ag, Cs, Tl, Pb, Th and U.

Isotopes analysed with *He mode* were Mg, Ca, Ni, Zn, Ga, As, Rb, Sr, Cd and Ba. *He mode* was the ones respect to the other gas available (hydrogen and oxygen) that provided best results according to a high determination coefficient in the related calibration curve. The optimized parameters were: 3 replicates, 90 sweeps/replicate, 3 points for peak pattern and integration time between 0.30 and 3 s.

LOD for the instrument carrier solution are listed in table S1 (supplementary materials) and expressed in parts per billion (ppb). LOD parameter has the lowest value for Ag and U with 0.001 ng mL^{-1} and the highest ones for Al and P with 2.170 ng mL^{-1} and 1.520 ng mL^{-1} respectively.

LOD of the process has the lowest value again for Ag, U with also Tl with 0.002 ng mL^{-1} while the highest value is 1.440 ng mL^{-1} for P and 1.370 ng mL^{-1} for K.

Linearity. External calibration curve was created on 8 points in parts per billion (ppb): 0.1 ppb, 0.5 ppb, 1 ppb, 5 ppb, 10 ppb, 50 ppb, 100 ppb, and 150 ppb. The linearity of the curve was estimated through the R^2 correlation coefficient for each element of the multi-standard solution as reported in table S1, together with the isotope of the element, the gas mode analysis, in a range of calibration between 0.1 and 150 ng mL^{-1}. The calibration curve results are strongly linear for each element, with the highest R^2 number for Be, Rb, Cd, Th and U with a determination coefficient of 1.000 and the lowest obtained for Ca and Fe with a determination coefficient of 0.9995.

Accuracy. The SRM-1573A was used for the determination of B, Na, Mg, Al, P, K, Ca, Mn, Fe, Co, Rb, Sr, Cd and Ba. Considering that not all the elements included in multi-element standard solution were present in the SRM-1573A, spiked multi-element standard addition of 2 ml was made to grant an efficient recovery, thus enabling a robust accuracy analysis also for Be, V, Cr, Ni, Cu, Zn, Ga, As, Se, Ag, Cs, Tl, Pb, Th and U. The volume addition of spiked standards with SRM-1573A was calculated to yield 16 ppb of each element's concentration in the final sample solution. In table S1 recovery results are reported with relative standard deviation (RSD) as percentage. The element listed with ∗ represent the ones determined with the spiked standard additions. Both the SRM-1573A sample and the SRM-1573A with spiked standards addition were analysed with two different dilutions, 25 times (1:25) to better characterized the minor concentrations and 100 times (1:100) to better characterized the highest concentration under the prefixed concentration range. Recovery's value is high for Mg, K, Mn, Fe, Rb, Sr, with full recoveries of the elements. On the opposite, the lowest recovery value is the one of Ag with a recovery of 61.7%.

Repeatability parameter was validated with the reproduction of SRM-1573A sample coupled with multi-element IV-ICPMS-71A spiked standard addition. The analysis was reproduced five times within one day with three replicates for sample. Table S1 shows the mean concentration obtained for each element included into the multi-element standard solution expressed in ng mL^{-1} and the RSD in percentage. Each repetition was introduced into the instrument with two different dilutions, 25 times (1:25) and 100 times (1:100).

Inter-day repeatability parameter was validated with the reproduction of SRM-1573A with spiked standard addition within three days. Three different sample were reproduced from the accurate weigh of SRM-1573A through acid digestion. Each analysis was developed with two different sample dilution, 25 times (1:25) and 100 times (1:100). As reported in table S1 almost all the elements were analysed reproducing similar results during different days, thus assure results validity.

3.2. Validation method parameters for REE analysis

ICP-MS generally has detection limits that are the most conventional for REE covering mass range from 139 uma of La to 175 uma of Lu. Polyatomic ions often occur as interferences. Therefore, oxide ions from REEs are mostly potential spectral interferences for middle to heavy analysis. To overcome this overlapping, O_2 reactive gas is used giving higher detectability and selectivity in respect of the other reactive gases. The optimized parameters for REE analysis were the same used for multi-element trace analysis. Isotopes analysed with *no-gas* mode were Eu, Tb and Yb. Isotopes analysed with *O_2 mode* were La, Ce, Pr, Nd, Sm, Gd, Dy, Ho, Er, Tm and Lu. Not all the elements are analysed in *O_2 mode*, due to the non-reactivity with O_2.

LOD and LOQ for the instrument were calculated on each element's standard deviation obtained from the analysis of instrument carrier solution (Table S2 - supplementary materials). The lowest LOD parameter value were the ones of Eu, Tm and Lu with 0.017 ng mL^{-1}, 0.019 ng mL^{-1} and 0.013 ng mL^{-1} respectively. The highest one is reported for Nd with 0.170 ng mL^{-1}.

LOD and LOQ for the process were checked trough the analysis of acid mixture used for every sample mineralization (Table S2). Elements like Gd, Ho and Yb have LOD low values of 0.017 ng mL^{-1}, 0.011 ng mL^{-1} and 0.021 ng mL^{-1} respectively. LOD and LOQ values for Tm under detectable limit.

Linearity. REE calibration curve was realized with CMS-1 stock standard solution on 8 points in parts per trillion (ppt): 0.1 ppt, on 0.25 ppt, 0.5 ppt, 1.0 ppt, 5.0 ppt, 10 ppt, 25 ppt and 50 ppt. In table S2 it's reported each element analysed for ultra-trace analysis, with its relative isotope, instrument operation mode and correlation coefficient (R^2) resulted, in a range of calibration between 0.1 and 150 ng mL^{-1}. Clearly each element analysed presented high correlation coefficient, especially Pr, Sm, Eu, Gd, Dy, Ho, Er, Tm, Yb and Lu, whose correlation coefficient was 1.000.

Accuracy parameters was validated with each element concentration recovery from SRM-1573A utilization with spiked standard addition of CMS-1 stock standard solution. In order to check the efficiency of the analysis for REE elements, for recovery calculation were taken in consideration the concentrations added with the spiked standard, since ultra-trace elements concentrations in SRM were indicative and not suitable for an accurate measure. In table S2 are listed the percentages of elements recovery and their RSD to each element with its relative isotope. All the REE elements were fully recovered. Furthermore, percentages above 100% indicate the low concentration in SRM-1573A that was certified just for consultation purpose.

Repeatability was checked with the repetition of same analysis with three replicate each. SRM-1573A with spiked standard addition were digested and analysed five times. Results are reported in table S2 through the main concentration obtained expressed in ng L-1 and RSD in percentage. Around 40 ppt of each REE was introduced with the spiked standard addition. The mean concentration reported indicates a satisfactory mean concentration calculated from the five repetitions.

Inter-day repeatability parameter validation was realized preparing the same sample used for repeatability but within three days. Each day a new analysis was conducted. Results are shown in table S2. Taking in consideration the concentration contribution of the spiked standards, data reported mean not only solid reliability due to results repetition but also substantial consistency regarding value obtained.

3.3. EVO oil samples multi-element trace and REE analysis

To better visualize all multi-element and REE sample fingerprint results given, all the samples were grouped in four geographical zones: Central Italy, South Italy, Albany, and commercial COOP samples to characterize EVO oil from the different geographical areas. Central Italy includes Tuscany, Marche, and Liguria, while South Italy refers to Abruzzo, Calabria, Campania, Apulia, and Sardinia.

Generally, the EVO oil from the south of Italy has higher value of multi-element and REE respect to the EVO oil from Central Italy (120 ppb and 40 ppb respectively for multi-element and 40 ppt and 25 ppt respectively for REE), as shown in Figure 2. Two samples of Albany EVO oil were analysed to have an idea of a foreign oil's mineral composition. It appears similar to mineral fingerprint obtained with Italian ones.

In detail, Figure 2a reports the multi-element results for Central Italy. Iron is the element most present (with a maximum value of 39.523 ppb), followed by P, Ca, Al and K. Besides their toxicological and nutritional importance, metals play an important role in the stability of olive oils and the presence of Fe, Cu, Cr and Mn was observed in various studies. All the samples collected in Central Italy show similar value, except for Fe and Ca, that are higher than those described by Beltrán et al. (2015) or Sayago et al. (2018). Also, Na and K value are higher respect to those described by Camin et al. (2010) or Zeiner et al. (2010), except for the Liguria EVO oil sample. On the other hand, levels of toxic elements such as As, Cd, Ni and Pb are significantly lower than those reported in other works (Camin et al., 2010, Zeiner et al., 2010; Karabagias et al., 2013, Sayago et al., 2018). Observing the EVO oil collected in Tuscany but from different years (2013 and 2014 in Fig. 2a), it is important to note that the sample from 2014 shows higher level of all the elements respect to sample from 2013, except for Ca, Cr and Zn. In addition, the concentration of Fe in the 2014 sample is the highest of all the other samples from the Central Italy (39.523 ppb, as previously described). The Fe data obtained are similar to than those reported by Cabrera-Vique et al. (2012), who found Fe concentrations between 3.350 and 66.470 µg kg-1 from Granada, Andalusia, Spain in virgin olive oils, but lower than those reported by Mendil et al. (2009) on olive oil from Turkey (Fe = 139.0 ± 10.1 µg g-1) and by Zeiner et al. (2010) on virgin olive oil from Croatia (Fe = 1.81 ± 1.76 µg g-1). These authors explained that these differences between elements content could be attributed to the geographical origin (Cabrera-Vique et al., 2012) and could be used for their local characterization. Other authors hypothesize that this difference may originate from fertilizers or contamination during processing and storage (Gouvinhas et al., 2016). Liguria EVO oil is the one that shows the lowest values in all elements (Fig. 2a).

Figure 2b illustrates ultra-trace REEs main composition of Central Italy samples. Ce, La and Nd are the most present element in the ultra-trace elements of EVO oil samples and the Liguria EVO oil (coloured in green in Fig. 2b) is the sample with the highest values of trace elements.

If compared Figure 2a with Figure 2c, it's noticeable how multi-element concentration levels are higher in EVO oils of South Italy (Fig. 2c), reaching elevated concentration for Fe with a maximum value in Abruzzo (2017) sample with 111.840 ppb. Apparently, the EVO oil samples from the south show a concentration more similar to each other, but the scale changes (here 120 ppb). The EVO oil samples from the south different, in fact, from each other in the concentration of Fe, Ni (Benincasa et al., 2007) but also in Al and K. Concentrations of Na found in these samples are in the range of 1.754 ppb (Sardinia) – 10.764 ppb (Calabria) which is similar to that found in Zeiner et al. (2010), Beltrán et al. (2015) or Benincasa et al. (2012) but 50 times lower than the levels reported in Portuguese olive oils (Gouvinhas et al., 2016). The concentrations of Mn measured is lower than 1 ppb, which is 10 times lower than those of olive oils from five different geographic regions of central and southern Italy (Rossano, Andria, Lamezia, Spoleto and Pescara) (Benincasa et al., 2007) and 100 times lower than that previously reported in Benincasa et al. (2012), but in a similar range than those of Italian olive oils from Sicily and Tuscany (Camin et al., 2010). Also in this samples, levels of toxic elements such as As, Cd, Ni and Pb are significantly lower than those reported in other works, as previously described. Observing the EVO oil samples collected in Campania but from different years (2015a, 2015b and 2017), it is important to note that the sample from 2017 shows higher level of the majority of the elements respect to sample from the two others, except for Na and Al, which show doubling values compared to those of 2017. In addition, the Calabria EVO oil sample collected in Crotone (2015a) shows high value of all the elements respect to the EVO oil samples collected in Castrovillari (2015b) and Rossano (2015c). Finally, in the Apulia samples no remarks are observed.

Also, for Figure 2d, it's easily noticeable how lanthanides concentration is higher for South Italy samples, reaching the highest values for two Calabria samples (2015a and 2015c, coloured in orange and yellow respectively).

The samples from Albany should have had similar concentrations, since the EVO oil was produced in same mill, from the same olives and plants. The 2014 EVO oil sample shows higher values in K, Ca, Fe, Ni, Zn, while the 2015 EVO oil sample in Na, Mg, Al, P and Sr (Fig. 2e). Generally, the Albany samples appear similar in concentration value to EVO oil sample from central Italy, but with the highest value of Ca as for other EVO oil samples from south of Europe, as for example in Spain (Sayago et al., 2018), Croatia (Zeiner et al., 2010), Greek (Karabagias et al., 2013).

As for multi-element analysis, the two samples from Albany appear similar in concentration value to EVO oil sample from Central Italy. Also in this case, the two Albany EVO oil samples show differences in the majority of the REE elements, but generally, the samples collected in 2015 has higher value respect to the sample collected in 2014 (Fig. 2f).

The three samples from COOP production show similar concentration of the central Italy and of the Albany EVO oil samples, with a maximum value of P and Fe around 30 ppb (Fig. 2g). Al and Ca are also present as for all other EVO oil samples.

The two COOP Fiore samples show similar value to each other for REE elements, this could confirm similar provenance (Fig. 2h). Different value, on the other side, has the EVO oil sample COOP Costanza, probably from different origin. Generally, REE values in COOP FIORE are similar to those from the Central Italy (except for the EVO oil from Liguria). The opposite is for the EVO oil COOP Costanza, which shows similar value on the EVO oil samples collected in Central Italy. Nevertheless, results in Figure 2h are different from results in Figure 2g, where the two COOP Fiore EVOOs are significantly different in the content of Na, Al, Fe and Zn, while the COOP Costanza EVOO has more similar concentration to one of them. All these considerations could give us a good information related to the possible provenance of the Italian EVO oil COOP FIORE and Costanza.

Scientific researchers have been reported that the content in mineral is usually affected in practice by the agro-environmental conditions and the olive genetic diversity (Gouvinhas et al., 2016), which certainly reflects the origin of provenance. The content of trace metals in EVO oil is also an important criterion for the assessment of oil quality with regard to their influence on human nutrition and health. Contents of Ni, As, Cu, Fe, Cd and Pb in all the samples analyzed are given in table 2. Especially As, Cd and Pb are very important on their toxicity and metabolic role because they catalyze the decomposition of hydro-peroxides, aldehydes, ketones, acids, and epoxides (Yassin et al., 2021). These compounds could increase carcinogenic effect especially on the digestive system by reacting with proteins and pigments present in the food (Ghane et al., 2022).

Obtained results reveal that the highest detected content of Ni is registered in the Abruzzo 2017 EVO oil sample (28.971 ppb). Generally, the Apulia samples have high value of Ni, around 3 and 4 ppb. It is interesting to note that the Ni concentration in the same EVO oil but with different year of production show different value of this metal, for example Apulia with very different concentration of Ni and Tuscany 2013 and 2014 with Ni value 0.305 ppb and 2.517 ppb respectively. The sample Calabria 2015a came from Crotone and it shows higher value of contaminants respect to the other Calabria samples collected in the same year but in two small town respect to Crotone. This could be correlate to the higher pollution of the Crotone city that could affect the olive plant and consequently the oil. Instead of the Ni value of the two sample of Campania EVO oil is very similar. All these values are lower than other EVO oil samples, for example compared to the Iranian EVO oil (Ziarati et al., 2019). The highest content of As is registered in the Campania 2017 sample, but generally with very low value in all the samples analyzed. Table 2 shows also the Cd content, for which the highest value is registered in the Campania 2017 sample as for As content, but also in this case lower than those other EVO oil samples (Ziarati et al., 2019). In addition, the highest Pb concentration is registered in Calabria 2015a and Apulia 2016 samples (range around 1 ppb, lower than those other EVO oil samples (La Pera et al., 2002; Ziarati et al., 2019). Finally, the concentrations of Cu measured is 0.35 ppb both for the samples collected to the north and to the south of Italy. This value is much lower than those previously reported in Argentine (Savio et al., 2014), Spain (Cabrera-Vique et al., 2012) and Italy too (Astolfi et al., 2021). Nevertheless, these results confirm that the contents of Ni, As, Cd and Pb in all the Italian samples analyzed not exceed the limits set by Codex Alimentarius and USDA (2001) and by the International Olive Oil Council (2009) related the legislated metals (As, Cu, Fe and Pb). The average contents of V in the EVO oil samples are 0.259 and 0.296 for the north samples and the south samples respectively and are significantly lower than in European EVO oil (Beltrán et al., 2015; Llorent-Martínez et al., 2011a; Pošćić et al., 2019) but also in the other Italian study, as in Astolfi et al. (2021), in which the average V value is equal to 0.52 in the Italian EVO oil samples.

By comparing our data with those of the other scientific research, generally, REE trace elements are detected in similar quantities than those previously reported by Sayago et al. (2018) and in greater quantity than those reported by Camin et al. (2010). Moreover, some correlations between REEs are found as shown in Figure 3, Ce, Nd and Gd are correlated in all samples analysed. Ce and Nd are also ones of the most REEs concentrated (Fig. 3a), with a maximum of

36.986 ppt and 14.938 ppt respectively in Calabria (2015c) sample. In addition, also La-Nd and La-Sm (Figs. 3d and 3e respectively) have correlated each other but lower respect to the previous elements described.

Table 2. Content of toxic metals in the various samples collected and analyzed by ICP-MS-QQQ, expressed in ppb.

Sample name	Ni	As	Cu	Fe	Cd	Pb
Albany 2014	0.140 x10	0.050	0.493	0.179 x 10^2	0.017	0.442
Albany 2015	0.217	0.127	0.277	0.158 x 10^2	0.000	0.006
Tuscany 2013	0.305	0.023	0.467	0.153 x 10^2	0.006	0.220
Tuscany 2014	0.251 x 10	0.009	0.375	0.395 x 10^2	0.002	0.468
Marche 2015	0.127 x 10	0.077	0.594	0.197 x 10^2	0.026	0.772
Liguria 2018	0.410	0.135	0.000	0.168 x 10^2	0.002	0.047
Abruzzo 2017	0.289 x10^2	0.082	0.445	0.111 x 10^3	0.004	0.180
Calabria 2015a	0.281 x 10	0.009	0.519	0.526 x 10^2	0.132	0.166 x 10
Calabria 2015b	0.563	0.000	0.457	0.148 x 10^2	0.051	0.618
Calabria 2015c	0.640	0.000	0.124	0.134 x 10^2	0.000	0.023
Campania 2015a	0.109 x 10	0.027	0.118	0.170 x 10^2	0.004	0.066
Campania 2015b	0.618 x 10	0.014	0.396	0.582 x 10^2	0.021	0.668
Campania 2017	0.885	0.431	0.353	0.145 x 10^2	0.308	0.435
Sardinia 2016	0.300	0.000	0.121	0.134 x 10^2	0.000	0.044
Apulia 2013a	0.327 x 10	0.032	0.456	0.206 x 10^2	0.009	0.382
Apulia 2013b	0.538	0.045	0.536	0.173 x 10^2	0.006	0.207
Apulia 2013c	0.174 x 10	0.073	0.222	0.248 x 10^2	0.004	0.130
Apulia 2014	0.350 x 10	0.023	0.238	0.233 x 10^2	0.000	0.522
Apulia 2016	0.233 x 10	0.005	0.529	0.414 x 10^2	0.049	0.147 x 10
Apulia 2018a	0.420 x 10	0.023	0.579	0.782 x 10^2	0.011	0.367
Apulia 2018b	0.359	0.200	0.159	0.125 x 10^2	0.132	0.129
Coop FIORE 2013	0.105 x 10	0.054	0.118 x 10	0.302 x 10^2	0.011	0.231
Coop FIORE 2014	0.487	0.049	0.000	0.123 x 10^2	0.002	0.032
Coop Costanza	0.156	0.077	0.000	0.126 x 10^2	0.004	0.031

3.4. Multivariate analysis

PCA was applied for a preliminary evaluation of data quality. In PCA analysis, eigenvalues represent the variance associated to the related principal component. The sum of all the eigenvalues is equal to the total variance of the data. Assuming that each eigenvalue < 1 is associated to the lowest relevant information, they could be eliminated without consequences. To do that, the first eight principal components with each eigenvalue, the variability (expressed in percent) and the cumulative variance (expressed in percent) are reported in table S3 (supplementary materials) and in the Scree Plot in Fig. S1 (supplementary materials) to graphically represent each component weight on the total variance. Table S3 reflects the quality of the projections from the N-dimensional initial table to a lower number of dimensions. First eigenvalue equals to 15.004 represents the 36.6% of the system variance. Observing PC1 and PC2 cumulative variance, the first two principal components represent 60.4% of the initial variability. PC1 represent the maximum variance, and being orthogonal with PC2 for construction, is uncorrelated with it. PC2 represents the maximum residual variance. Scree plot graphs eigenvalues in function of PC's number (Fig. S1). The selection of PCs is made according to a sharp decrease of the curve to the horizontal asymptote. The distinction of the first two PCs is already graphically clear compared to the following others.

Then, to analyse graphically the variables' role, a PCA loadings plot is required. In Figure S2 (supplementary materials) a correlation circle is reported, which described not a confidence interval but a plot of the correlation between the variables and the principal components (PC1 and PC2). Horizontal axis represents PC1 and vertical axis PC2, while the red vectors reflect the investigated variables. According to the length of each vector, it's explained the

representativeness quality in the investigated PCA dimensions; longer a vector is more it's represented by these two principal components. The shortest ones might be better explained from other factors (Popović et al., 2020). REEs are well represented from PC1 reporting La, Ce, Pr, Nd, Sm, Eu, Gd, Tb, Dy, Ho, Er, Tm, Yb and Lu. REEs form a right angle with some of the contaminants well represented from PC2, denoting that are uncorrelated to each other. Contaminants reported in PC2 axis are Cd, As, V, Ba, Tl, Th and U. This is more important, because these contaminants generally enter into the soil agro-ecosystem through natural processes and anthropogenic activities (Li et al., 2019; Mng'ong'o et al., 2021). In detail, Cd is one of the toxic metals most monitored, due to its relevant consequences on human health, and it is transferred to food through fertilizers, in particular the ones based on P, and through packaging systems (Osman et al., 2019). The concentration of Cd in phosphate fertilizers is an issue of great concern and its allowed amount has been continuously discussed by European Commission (Ulrich, 2019); its presence has been found in phosphoric pentoxide due to Cd trace concentration in the phosphate rock used for their manufacture (Zheng et al., 2020; Liu et al., 2021). Almost all phosphate fertilizers are produced from phosphate rock (El-Bahi et al., 2017). Moreover, Cd contamination from fertilizers is mainly accumulated in crop-production soil sand its accumulation might be higher in south Mediterranean soils, where rains are less frequent, thus obstructing its leaching (Nardi et al., 2017; El-Sherbiny and Sallam, 2021). In Fig. S2, Cd is relevant in the analysis of the PCA loadings plot. Knowing the low contamination on the geographically sampling site not so close to important route (except only for one site), the high value of this contaminant could be related to agronomic practices through the use of phosphate fertilizers (Dharma-wardana, 2018; Schaefer et al., 2020). Another element that can be introduced easily into food chain is As, whose distribution has been defined from European Food Safety Authority mostly present in food commodities and current water (European Food Safety Authority, 2014) and it could be present in some pesticide's composition (Osman et al., 2019). In pesticides also Ba is traceable. In Fig. S2, As and Ba, as for Cd previously described, are relevant in the analysis of the PCA loadings plot. This could confirm a possible pollution by aggressive agronomic practices. Additionally, V is accumulated in soil composition, and it may cause a serious damage for crop cultivations, even if it is naturally present also into plant's tissues (Li et al., 2020). The diffusion of V into the atmosphere and subsequently its deposition in soil, is often due to anthropic reasons, since it is mainly released from oil's products combustion and from activities related to steel industry. Vanadium's anthropic emissions exceed natural ones by a factor of 1.7 (Schlesinger et al., 2017). In the PCA loadings plot of Fig. S2, V is not so important as the previous contaminants, but its presence adds importance to the possibility of anthropic contamination (Beltrán et al., 2015). These elements differed from metals like Ni, Cu, Zn and Pb, whose concentrations were constant in EVO oil samples. Moreover, at low concentrations toxic metals like Ni, Cu and Zn are micro-elements essential to the metabolic role and the reproduction of plants, animal, and humans (Hussain et al., 2020).

On the other hand, PCA score plot reports the separation among the EVO oil samples in relation to quality, cultivar, and processing method. Figure S3 (supplementary materials) presents the graphic distribution of the EVO oil samples in relation to the geographically origin, according to the first two principal components scores (PC1 and PC2). Each point of the graph is coloured according to their provenance origin. Most of the EVO oil samples are grouped in the lower part of the graph, except for the sample from Campania (Perdifumo – SA, 2015) and Apulia (Molfetta – BA, 2018b). The EVO oil samples from Calabria and Albany follow a different trend: the two samples of Albany seem to be in two different quadrants, even if always in the lower part of the graph (2014 in the left part and 2015 in the right part); while the EVO oil samples of Calabria, as well as being in different quadrants, are also found in different positions with respect to the zero of both PC1 and PC2. Finally, the sample of Liguria is found together with a sample of the Campania (Valturara – AV, 2017) and the two remaining ones of Calabria (Crotone – CR, 2015a and Rossano – CS, 2015c) in the upper right quadrant (opposite quadrant with respect to the quadrant in which most of the samples are found). A particular case is that of Sardinia, which together with a sample of Campania (Pimonte – NA, 2015) are found in the central part of the graph, where the 0 vectors of both PC1 and PC2 intersect. The graph in figure S3 allows discriminating EVO oil samples on the basis of the graphic distribution of the EVO oil samples in relation to the geographically origin, according to the elements quantify by the ICP-MS-QQQ analysis. EVO oil samples from the same geographical origin are very closed to each other, except for the Campania EVO oil samples, and especially for the two Campania EVO oil samples collected in the same place but in different years. This could be an important base for future study, to better characterize the sampling area to know change on soil or on plant maybe in relation to climate change or to different use of fertilizer.

To complete PCA analysis, a biplot is reported in Figure 4. The cluster in the negative side of PC1 and PC2 (on the left bottom of the graph in Fig. 4) represents samples characterized by high value of the general elements present in an EVO oil samples, as Zn, Cu and mostly Fe, as we expected (Martinez et al., 2018). In the biplot it's clear how two samples fall back into the contaminants area having higher concentrations of toxic elements compared to the others (Campania, Perdifumo – SA, 2015; Apulia (Molfetta – BA, 2013c). In the ones reported in the axis related to REEs elements are samples that stand out of the crowd for their particular high definition of ultra-trace composition of rare earth elements.

Regarding the three industrial olive oil samples, the two COOP Fiore (2013 and 2014) are very similar to most of the samples analysed. On the opposite, COOP Costanza is in the same part of the figure of Calabria and Liguria samples, but with higher value of REE elements.

4. Conclusion

This work focused on the research of a reliable method to analyse many EVO oil samples from different areas.

Fundamental steps of this method's development were sample's mineralization and sample's analysis. For the first one different acid mixtures were tested in order to use the minimum quantity of acid having at the same time a clear solution without any organic matrix dispersed in the solution. For the analysis step different dilutions were tested in order to obtain a sample reading suitable with a calibration curve calculated to contain each element's range of concentration. Moreover, the method developed was successfully validated according to some parameters that must be optimized to realize a reliable method: linearity, accuracy, LOD and LOQ, repeatability and inter-day repeatability.

In addition, using the triple quadrupole ICP-MS in a Clean Room ISO 6 significantly lowers the LODs of each elements analysed. This makes it possible to quantify even very low values or closed to the LOD, especially of REE, which can be excellent markers for identifying the fingerprint.

Good results were obtained both for trace multi-element analysis and for ultra-trace REE analysis as we expected. Both trace and ultra-trace elements show changes between the analysed samples.

At the end, with data obtained from trace (ppb) and ultra-trace (ppt) analysis a PCA was conducted to start pointing out a possible and continuative study on the relationship between EVO oil samples, originating from different areas.

References

Aceto, M., Bonello, F., Musso, D., Tsolakis, C., Cassino, C., & Osella, D. (2018). Wine Traceability with Rare Earth Elements. *Beverages*, *4*, 23. https://doi.org/10.3390/beverages4010023

Astolfi, M. L., Marconi, E., Vitiello, G., & Massimi, L. (2021). An optimized method for sample preparation and elemental analysis of extra-virgin olive oil by inductively coupled plasma mass spectrometry. *Food Chemistry*, *360*, 130027. https://doi.org/10.1016/j.foodchem.2021.130027

Beltrán, M., Sánchez-Astudillo, M., Aparicio, R., & García-González, D. L. (2015). Geographical traceability of virgin olive oils from south-western Spain by their multi-elemental composition. *Food Chemistry*, *169*, 350-357. https://doi.org/10.1016/j.foodchem.2014.07.104

Benincasa, C., Lewis, J., Perri, E., Sindona, G., & Tagarelli, A. (2007). Determination of trace element in Italian virgin olive oils and their characterization according to geographical origin by statistical analysis. *Analytica Chimica Acta*, *585*, 366-370. https://doi.org/10.1016/j.aca.2006.12.040

Benincasa, C., Gharsallaoui, M., Perri, E., Bati, C. B., Ayadi, M., Khlif, M., & Gabsi, S. (2012). Quality and trace element profile of Tunisian olive oils obtained from plants irrigated with treated wastewater. *The Scientific World Journal*, *2012*, 1-11. https://doi.org/10.1100/2012/535781

Cabrera-Vique, C., Bouzas, P. R., & Oliveras-Lopez, M. J. (2012). Determination of trace elements in extra virgin olive oils: A pilot study on the geographical characterisation. *Food Chemistry*, *134*, 434-439. https://doi.org/10.1016/j.foodchem.2012.02.088

Camin, F., Larcher, R., Perini, M., Bontempo, L., Bertoldi, D., Gagliano, G., Nicolini, G., & Versini, G. (2010). Characterisation of authentic Italian extra-virgin olive oils by stable isotope ratios of C, O and H and mineral composition. *Food Chemistry*, *118*, 901-909. https://doi.org/10.1016/j.foodchem.2008.04.059

Codex Alimentarius Commission (2001) Report of the 33rd session of the codex committee on food additives and contaminants. Rome, Italy: Food and Agriculture Organization of the United Nations/World Health Organization.

Damak, F., Asano, M., Baba, K., Suda, A., Araoka, D., Wali, A., Isoda, H., Nakajima, M., Ksibi, M., & Tamura, K. (2019). Interregional traceability of Tunisian olive oils to the provenance soil by multielemental fingerprinting and chemometrics. *Food Chemistry*, *283*, 656-664. https://doi.org/10.1016/j.foodchem.2019.01.082

Dharma-Wardana, M. W. C. (2018). Fertilizer usage and cadmium in soils, crops and food. *Environmental Geochemistry and Health*, *40*, 2739-2759. https://doi.org/10.1007/s10653-018-0140-x

El-Bahi, S. M., Sroor, A., Mohamed, G. Y., & El-Gendy, N. S. (2017). Radiological impact of natural radioactivity in Egyptian phosphate rocks, phosphogypsum and phosphate fertilizers. *Applied Radiation and Isotopes*, *123*, 121-127. https://doi.org/10.1016/j.apradiso.2017.02.031

El-Sherbiny, H. M. M., & Sallam, K. I. (2021). Residual contents and health risk assessment of mercury, lead and cadmium in sardine and mackerel from the Mediterranean Sea Coast, Egypt. *Journal of Food Composition and Analysis*, *96*, 103749. https://doi.org/10.1016/j.jfca.2020.103749

European Commission (2020). Quality Schemes explained. https://ec.europa.eu/info/food-farming-fisheries/food-safety-and-quality/certification/quality-labels/quality-schemes-explained_en

European Food Safety Authority (2014). Dietary exposure to inorganic arsenic in Euro pean population. *EFSA Journal*, *12*, 3597. https://doi.org/10.2903/j.efsa.2014.3597

Ghane, E. T., Poormohammadi, A., Khazaei, S., & Mehri, F. (2022). Concentration of Potentially Toxic Elements in Vegetable Oils and Health Risk Assessment: a Systematic Review and Meta-analysis. *Biological Trace Element Research*, *200*, 437-446. https://doi.org/10.1007/s12011-021-02645-x

Gouvinhas, I., Dominguez-Perles, R., Machado, N., Carvalho, T., Matos, C., & Barros, A. I. R. N. A. (2016). Effect of agro-environmental factors on the mineral content of olive oils: Categorization of the three major portuguese cultivars. *Journal of the American Oil Chemists' Society*, *93*, 813-822. https://doi.org/10.1007/s11746-016-2827-4

Hussain, S., Khaliq, A., Noor, M. A., Tanveer, M., Hussain, H. A., Hussain, S., Shah, T., & Mehmood, T. (2020). Metal Toxicity and Nitrogen Metabolism in Plants: An Overview. In: Datta R., Meena R., Pathan S., Ceccherini M. (eds) Carbon and Nitrogen Cycling in Soil. Springer, Singapore. https://doi.org/10.1007/978-981-13-7264-3_7

International Olive Council (2009). Trade standard applying to olive oils and olive-pomace oils. COI/T.15/NC No. 3/Rev.

Karabagias, I., Michos, C., Badeka, A., Kontakos, C., Stratis, I., & Kontominas, M. G. (2013). Classification of Western Greek virgin olive oils according to geographical origin based on chromatographic, spectroscopic, conventional and chemometric analyses. *Food Research International*, *54*, 1950-1958. https://doi.org/10.1016/j.foodres.2013.09.023

La Pera, L., Lo Curto, S., Visco, A., La Torre, L., & Dugo, G. (2002). Derivative Potentiometric Stripping Analysis (dPSA) Used for the Determination of Cadmium, Copper, Lead, and Zinc in Sicilian Olive Oils. *Journal of Agricultural and Food Chemistry*, *50*, 3090-3093. https://doi.org/10.1021/jf0113124

Li, C., Zhou, K., Qin, W., Tian, C., Qi, M., & Yan, X. (2019). A review on heavy metal contamination in soil: Effects, Sources and Remediation techniques. *Soil and Sediment Contamination: An International Journal*, *28*, 380-394. https://doi.org/10.1080/15320383.2019.1592108

Li, Y., Zhang, B., Liu, Z., Wang, S., Yoa, J., & Borthwick, A. G. L. (2020). Vanadium contamination and associated health risk of farmland soil near smelters throughout China. *Environmental Pollution*, *263*, 114540. https://doi.org/10.1016/j.envpol.2020.114540

Liu, B., He, Z., Liu, R., Montenegro, A. C., Ellis, M., Li, Q., & Baligar, V. C. (2021). Comparative effectiveness of activated dolomite phosphate rock and biochar for immobilizing cadmium and lead in soils. *Chemosphere*, *266*, 129202. https://doi.org/10.1016/j.chemosphere.2020.129202

Llorent-Martınez, E. J., Ortega-Barrales, P., Fernadez-de Cordova, M. L., Dominguez-Vidal, A., & Ruiz-Medina, A. (2011). Investigation by ICP-MS of trace element levels in vegetable edible oils produced in Spain. *Food Chemistry*, *127*, 1257-1262. https://doi.org/10.1016/j.foodchem.2011.01.064

Martínez, L., Ros, G., & Nieto, G. (2018). Fe, Zn and Se Bioavailability in Chicken Meat Emulsions Enriched with Minerals, Hydroxytyrosol and Extra Virgin Olive Oil as Measured by Caco-2 Cell Model. *Nutrients*, *10*, 969. https://doi.org/10.3390/nu10080969

Mendil, D., Ozgur, D. U., & Mustafa, S. (2009). Investigation of the levels of some element in edible oil samples produced in Turkey by atomic absorption spectrometry. *Journal of Hazardous Materials*, *165*, 724-728. https://doi.org/10.1016/j.jhazmat.2008.10.046

Mng'ong'o, M., Munishi, L. K., Ndakidemi, P. A., Blake, W., Comber, S., & Hutchinson, T. H. (2021). Toxic metals in East African agro-ecosystems: Key risks for sustainable food production. *Journal of Environmental Management*, *294*, 112973. https://doi.org/10.1016/j.jenvman.2021.112973

Nardi, A., Mincarelli, L. F., Benedetti, M., Fattorini, D., d'Errico, G., & Regoli, F. (2017). Indirect effects of climate changes on cadmium bioavailability and biological effects in the Mediterranean mussel Mytilus galloprovincialis. *Chemosphere*, *169*, 493-502. https://doi.org/10.1016/j.chemosphere.2016.11.093

Osman, M. A., Yang, F., & Massey, I. Y. (2019). Exposure routes and health effects of heavy metals on children. *Biometals*, *32*, 563-573. https://doi.org/10.1007/s10534-019-00193-5

Popović, B. M., Blagojević, B., Ždero Pavlović, R., Mićić, N., Bijelić, S., Bogdanović, B., Mišan, A., Duarte, C. M. M., & Serra, A. T. (2020). Comparison between polyphenol profile and bioactive response in blackthorn (Prunus spinosa L.) genotypes from north Serbia-from raw data to PCA analysis. *Food Chemistry*, *302*, 125373. https://doi.org/10.1016/j.foodchem.2019.125373

Rizzo, A., & Telloli, C. (2019). Analytical techniques for a rapid determination of nitrogen content in Extra Virgin Olive Oil. *Journal of Agronomy and Agricultural Science*, *1*, 1-5. https://doi.org/10.24966/AAS-8292/100005

Savio, M., Ortiz, M. S., Almeida, C. A., Olsina, R. A., Martinez, L. D., & Gil, R. A. (2014). Multielemental analysis in vegetable edible oils by inductively coupled plasma mass spectrometry after solubilisation with tetramethylammonium hydroxide. *Food Chemistry*, *159*, 433-438. https://doi.org/10.1016/j.foodchem.2014.03.041

Sayago, A., González-Domínguez, R., Beltrán, R., & Fernández-Recamales, A. (2018). Combination of complementary data mining methods for geographical characterization of extra virgin olive oils based on mineral composition. *Food Chemistry*, *261*, 42-50. https://doi.org/10.1016/j.foodchem.2018.04.019

Schaefer, H. R., Dennis, S., & Fitzpatrick, S. (2020). Cadmium: Mitigation strategies to reduce dietary exposure. *Journal of Food Science*, *85*, 260-267. https://doi.org/10.1111/1750-3841.14997

Schlesinger, W. H., Klein, E. M., & Vengosh, A. (2017). Global biogeochemical cycle of Vanadium. *Proceedings of the National Academy of Sciences*, *114*, E11092-E11100. https://doi.org/10.1073/pnas.1715500114

Ulrich, A. E. (2019). Cadmium governance in Europe's phosphate fertilizers: Not so fast? *Science of the Total Environment*, *650*, 541-545. https://doi.org/10.1016/j.scitotenv.2018.09.014

Yassin, A. A., Ghandour, M. A., & Khalil, M. M. (2021). Health risk assessment and micro determination of trace elements content in Egyptian olive oil using ICP-OES. *IOP Conference Series: Materials Science and Engineering*, *101*, 22-32.

Zeiner, M., Juranovic-Cindric, I., & Škevin, D. (2010). Characterization of extra virgin olive oils derived from the Croatian cultivar Oblica. *European Journal of Lipid Science and Technology*, *112*, 1248-1252. https://doi.org/10.1002/ejlt.201000006

Zheng, G., Wang, X., Chen, T., Yang, J., Yang, J., Liu, J., & Shi, X. (2020). Passivation of lead and cadmium and increase of the nutrient content during sewage sludge composting by phosphate amendments. *Environmental Research*, *185*, 109431. https://doi.org/10.1016/j.envres.2020.109431

Ziarati, P., Mirmohammad Makki, F., Vambol, S., & Vambol, V. (2019). Determination of Toxic Metals Content in Iranian and Italian Flavoured Olive Oil. *Acta Technologica Agriculturae*, *2*, 64-69. https://doi.org/10.2478/ata-2019-0012

Supplementary materials

Table S1. LOD and LOQ of the instrument and of the process for multi-element trace analysis, expressed in ng mL^{-1}; linearity of the external calibration for multi-element trace analysis; accuracy determination trough SRM-1573A recovery and spiked standard additions; repeatability and inter-day repeatability of the multi element trace analysis. Symbol * represent element read at the higher dilution; symbol ° represent element read at (1:100) dilution.

	Instrument		***Process***		***Linearity***		***Accuracy***		***Repeatability***		***Inter-day repeatability (ng mL^{-1})***					
Element	**LOD**	**LOQ**	**LOD**	**LOQ**	**Mode**	***R2***	**Recovery (%)**	**RSD (%)**	**Mean Concentration**	**RSD (%)**	**Day 1**	**RSD (%)**	**Day 2**	**RSD (%)**	**Day 3**	**RSD (%)**
^{9}Be*	0.006	0.020	0.004	0.0152	No Gas	1.000	86.1	3.9	13.726	0.067	16.288	0.5	16.036	1.0	16.304	0.1
^{11}B	0.208	0.693	0.145	0.483	No Gas	0.9996	92.3	1.3	15.010	0.732	16.147	1.0	17.107	0.9	16.189	1.4
^{23}Na	0.012	0.052	0.281	0.935	No Gas	0.9997	87.5	1.4	17.153	0.778	16.220	0.9	19.190	0.7	16.807	1.0
^{24}Mg°	0.122	0.407	0.133	0.443	He	0.9999	106.2	2.3	38.924	0.217	56.856	4.2	52.628	0.3	55.579	2.5
^{27}Al	2.170	7.232	0.875	2.918	No Gas	0.9999	90.2	3.9	28.468	0.616	22.024	0.8	23.041	5.4	28.903	2.0
^{31}P	1.520	5.065	1.440	4.796	No Gas	0.9998	98.7	5.7	44.122	0.009	53.490	0.7	53.911	1.5	54.720	0.7
^{39}K°	0.730	2.432	1.370	4.566	No Gas	0.9998	114.3	0.3	93.789	0.225	161.800	1.1	126.999	1.4	134.759	1.4
^{44}Ca°	0.819	2.730	1.192	3.976	He	0.9995	77.2	1.7	28.750	0.717	43.159	6.1	35.685	2.9	40.391	4.3
^{51}V*	0.213	0.710	0.144	0.479	No Gas	0.9999	95.5	1.3	15.194	0.122	17.741	2.1	16.967	1.1	17.520	1.2
^{52}Cr*	0.049	0.162	0.061	0.203	No Gas	0.9998	93.2	1.3	14.865	0.059	17.202	0.3	16.878	1.3	17.040	0.1
^{55}Mn	0.018	0.061	0.009	0.029	No Gas	0.9999	109.3	1.2	18.048	0.066	20.922	0.5	20.667	1.2	21.017	0.6
^{56}Fe	0.520	1.730	0.460	1.533	No Gas	0.9995	110.6	3.1	21.994	0.217	24.514	1.8	23.625	1.3	24.938	0.5
^{59}Co	0.001	0.003	0.004	0.015	No Gas	0.9999	91.3	6.0	14.685	0.030	16.966	0.3	16.574	0.1	16.772	1.3
^{60}Ni*	0.040	0.130	0.164	0.550	He	0.9999	93.9	1.5	14.962	0.093	17.444	1.5	16.423	3.0	17.457	1.5
^{63}Cu*	0.012	0.041	0.070	0.232	No Gas	0.9997	89.4	1.0	14.295	0.008	16.607	0.4	16.231	0.6	16.547	0.4
^{66}Zn*	0.392	1.310	0.300	0.993	He	0.9999	62.6	4.6	9.771	0.346	15.809	0.6	15.284	4.6	15.629	3.4
^{69}Ga*	0.005	0.015	0.044	0.148	He	0.9999	94.0	1.5	15.021	0.037	16.838	1.5	16.980	1.6	17.360	2.0
^{75}As*	0.100	0.332	0.427	1.423	He	0.9999	92.0	2.9	14.674	0.075	16.459	4.6	15.790	2.7	16.169	1.0
^{78}Se*	0.338	1.126	0.173	0.575	No Gas	0.9999	82.9	4.9	13.172	0.134	15.538	2.6	16.191	3.1	15.397	3.7
^{85}Rb	0.019	0.065	0.035	0.120	He	1.0000	104.9	3.8	14.875	0.093	17.191	1.0	16.767	0.5	16.994	2.9
^{88}Sr	0.029	0.098	0.073	0.244	He	0.9999	106.9	1.0	15.674	0.160	18.241	2.1	18.441	1.4	18.328	0.2
^{107}Ag*	0.001	0.005	0.002	0.008	No Gas	0.9998	61.7	0.6	9.869	0.001	16.608	0.5	16.214	0.7	16.517	0.6

^{111}Cd	0.040	0.129	0.025	0.082	He	1.0000	81.0	3.3	14.497	0.123	16.350	1.6	16.718	2.2	16.821	3.4
^{133}Cs*	0.004	0.015	0.002	0.008	No Gas	0.9999	93.1	1.3	14.850	0.074	17.050	1.1	16.751	0.2	16.999	0.9
^{137}Ba	0.109	0.365	0.160	0.526	He	0.9998	98.8	0.5	15.205	0.127	17.837	3.9	18.407	3.3	17.749	3.3
^{205}Tl	0.002	0.006	0.002	0.005	No Gas	0.9998	85.6	0.7	13.682	0.030	15.728	0.8	15.482	0.2	15.736	0.7
^{208}Pb*	0.028	0.094	0.062	0.208	No Gas	0.9998	86.5	1.8	13.772	0.088	15.942	1.0	15.650	0.5	15.773	0.2
^{232}Th*	0.025	0.083	0.030	0.098	No Gas	1.0000	88.5	0.5	14.085	0.099	16.189	0.9	15.935	0.7	16.108	0.7
^{238}U*	0.001	0.004	0.002	0.005	No Gas	1.0000	88.5	0.7	13.888	0.033	17.037	1.9	16.404	3.5	16.096	1.4

Table S2. LOD and LOQ of the instrument and of the process for the rare earth elements (REE) ultra-trace analysis, expressed in ppt (n.d. means under detectable limit); linearity of the external calibration for the rare earth elements ultra-trace analysis (ppt); accuracy determination trough SRM-1573A recovery and spiked standard additions; repeatability and inter-day repeatability of the rare earth elements ultra-trace analysis.

	Instrument		***Process***		***Linearity***		***Accuracy***		***Repeatability***		***Inter-day repeatability (ppt)***					
Element	**LOD**	**LOQ**	**LOD**	**LOQ**	**Mode**	***R*2**	**Recovery (%)**	**RSD (%)**	**Mean Concentration**	**RSD (%)**	**Day 1**	**RSD (%)**	**Day 2**	**RSD (%)**	**Day 3**	**RSD (%)**
^{139}La	0.042	0.140	0.136	0.454	O_2	0.9999	104.3	1.7	42.303	1.7	42.069	2.1	41.475	2.2	41.705	1.7
^{140}Ce	0.042	0.141	0.093	0.311	O_2	0.9999	100.7	2.6	41.646	2.5	41.444	2.8	40.785	2.7	40.291	2.6
^{141}Pr	0.041	0.138	0.105	0.350	O_2	1.0000	105.7	2.3	42.786	1.6	42.689	0.6	41.958	2.1	42.302	2.3
^{146}Nd	0.170	0.568	0.469	1.565	O_2	0.9999	106.2	1.9	43.096	1.8	42.852	3.7	42.063	2.4	42.508	1.9
^{147}Sm	0.107	0.356	0.207	0.690	O_2	1.0000	103.9	2.7	42.583	2.3	42.860	2.5	41.512	1.5	41.544	2.7
^{153}Eu	0.017	0.057	0.032	0.107	No Gas	1.0000	106.9	0.3	43.238	2.0	43.599	0.5	42.055	2.2	42.776	0.3
^{157}Gd	0.068	0.228	0.017	0.057	O_2	1.0000	105.1	3.0	42.340	1.3	43.235	2.5	41.690	0.6	42.054	3.0
^{159}Tb	0.067	0.225	0.119	0.396	No Gas	0.9998	106.2	7.4	41.926	2.0	42.645	7.0	41.644	1.3	42.494	7.1
^{163}Dy	0.021	0.071	0.066	0.220	O_2	1.0000	106.2	2.9	43.241	1.7	42.748	2.1	42.673	1.7	42.483	2.9
^{165}Ho	0.036	0.012	0.011	0.037	O_2	1.0000	105.9	3.2	42.950	1.6	43.253	0.8	42.131	2.0	42.355	3.2
^{166}Er	0.061	0.202	0.068	0.228	O_2	1.0000	106.9	1.6	42.816	2.0	42.294	2.4	41.403	1.7	42.759	1.6
^{169}Tm	0.019	0.062	n.d.	n.d.	O_2	1.0000	106.4	1.0	43.046	1.7	43.187	0.4	41.900	2.0	43.383	0.9
^{172}Yb	0.049	0,164	0.021	0.070	No Gas	1.0000	105.6	0.5	43.004	1.3	43.501	1.1	42.854	1.1	42.039	0.9
^{175}Lu	0,013	0,045	0.650	2.166	O_2	1.0000	106.4	1.1	43.258	2.0	43.431	1.6	42.267	1.9	42.457	1.1

Table S3. Eigenvalues and cumulative variance (expressed in percentage) of the data obtained by ICP-MS-QQQ on EVO oil samples.

Principal Component	Eigenvalue	Variability (%)	Cumulative variance (%)
PC1	15.004	36.596	36.596
PC2	9.770	23.828	60.424
PC3	4.057	9.894	70.319
PC4	3.215	7.841	78.160
PC5	2.061	5.027	83.188
PC6	1.842	4.492	87.679
PC7	1.041	2.539	90.218
PC8	0.912	2.224	92.442

Figure S1

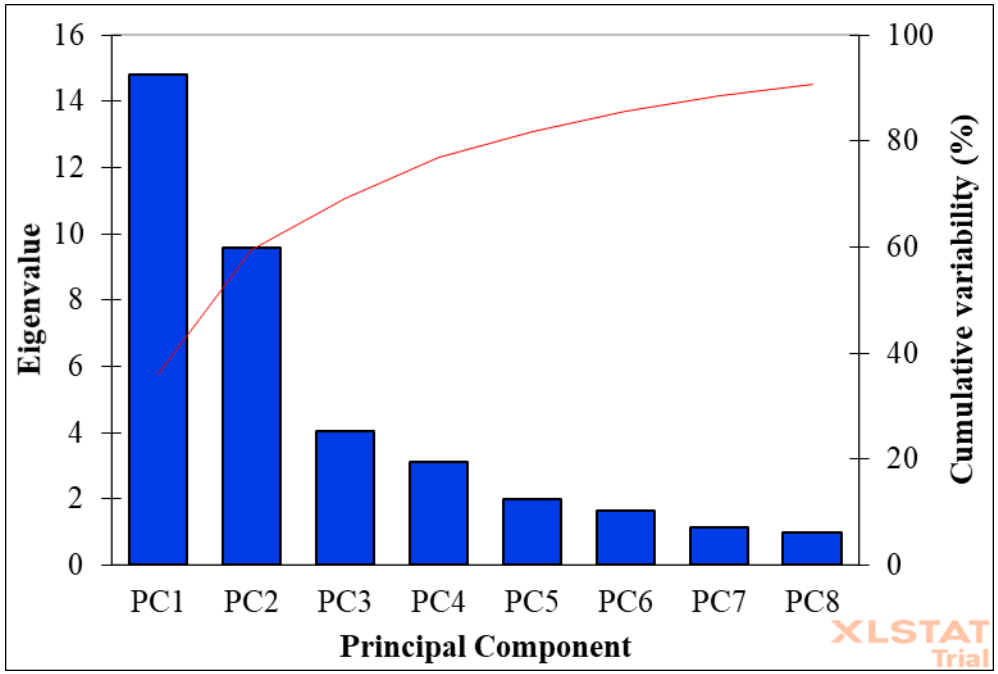

Figure S2

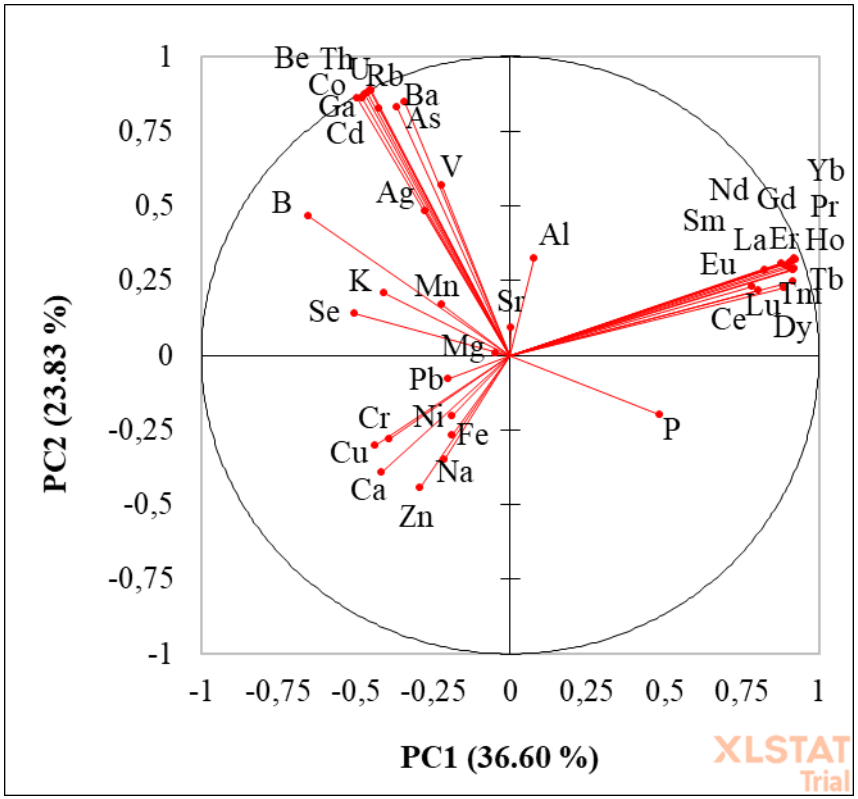
Be
Th
Co
U
Rb
Ba
Ga
As
Cd
V
Ag
B
Al
Yb
Nd
Gd
Pr
Sm
La
Er
Ho
Eu
Tb
K
Mn
Sr
Tm
Se
Ce
Lu
Dy
Mg
Pb
Cr
Ni
P
Cu
Fe
Na
Ca
Zn
1
0,75
0,5
0,25
0
-0,25
-0,5
-0,75
-1
-1
-0,75
-0,5
-0,25
0
0,25
0,5
0,75
1
PC2 (23.83 %)
PC1 (36.60 %)
XLSTAT
Trial

Figure S3

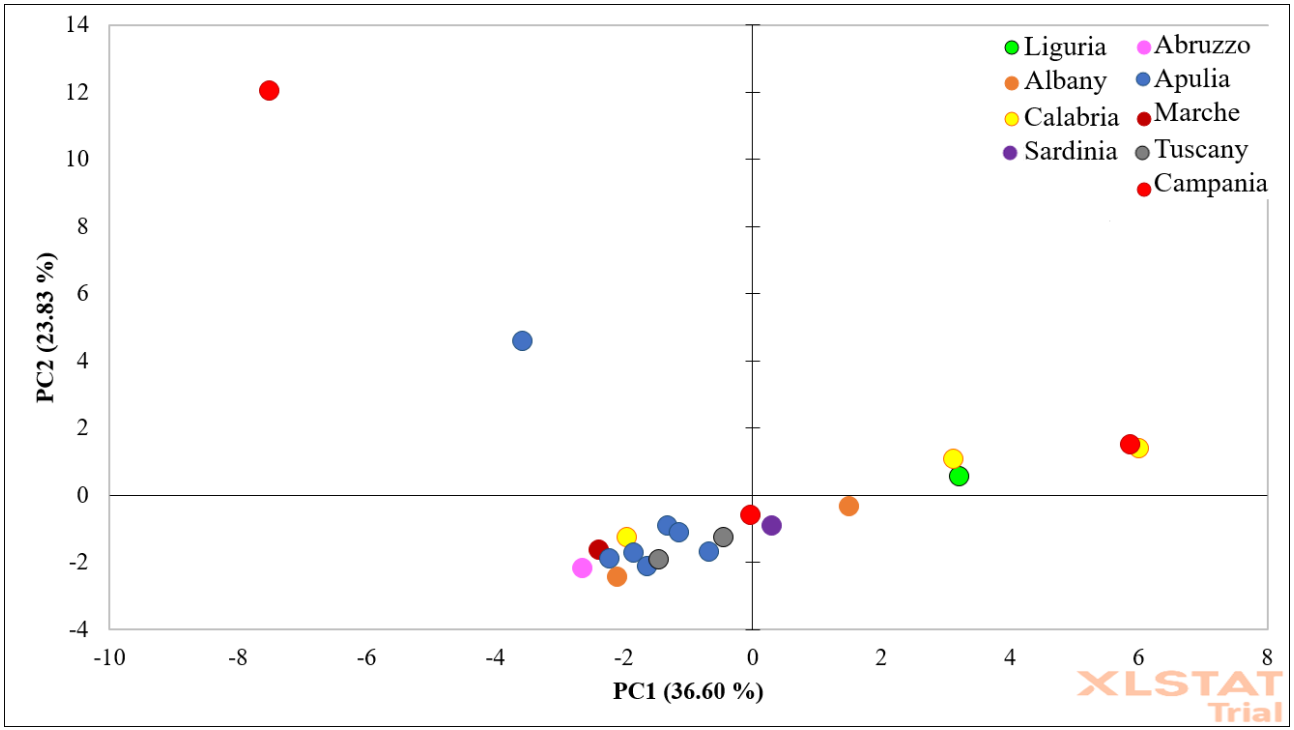
Liguria
Abruzzo
Albany
Apulia
Calabria
Marche
Sardinia
Tuscany
Campania
PC2 (23.83 %)
PC1 (36.60 %)
14
12
10
8
6
4
2
0
-2
-4
-10
-8
-6
-4
-2
0
2
4
6
8
XLSTAT
Trial

Figure captions

Figure 1. Extra Virgin Olive (EVO) oil sampling sites. On the right, some EVO oil after sampling collection.

Figure 2. Multi-element and REE ultra-trace data representation for EVO oil samples, expressed in ppb and ppt respectively: a) multi-element in Central Italy; b) REE in Central Italy; c) multi-element in South Italy; d) REE in South Italy; e) multi-element in Albany; f) REE in Albany; g) multi-element in COOP olive oil; h) REE in COOP olive oil.

Figure 3. REE regression in all the EVO oil samples, expressed in ppt, between a) Ce-Nd; b) Gd-Nd; c) Gd-Ce; d) La-Nd; e) La-Sm.

Figure 4. Principal Component Analysis (PCA) biplot of the EVO oil data obtained by ICP-MS-QQQ and analysed by XLstat Addinsoft. In black the three industrial olive oil samples. The red vectors reflect the investigated variables.

Figure S1. Scree plot related to Table S3 (supplementary materials), obtained with XLstat Addinsoft.

Figure S2. Principal Component Analysis (PCA) loadings plot of the EVO oil data obtained by ICP-MS-QQQ and analysed by XLstat Addinsoft. The red vectors reflect the investigated variables.

Figure S3. Principal Component Analysis (PCA) score plot of the EVO oil data obtained by ICP-MS-QQQ and analysed by XLstat Addinsoft.

Figures

Figure 1

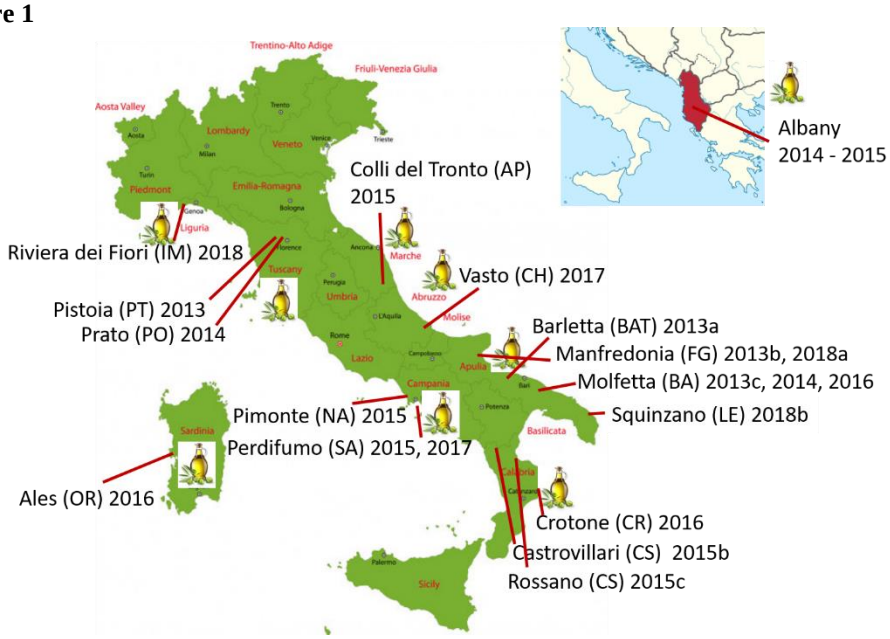

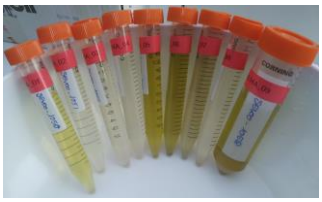

Figure 2

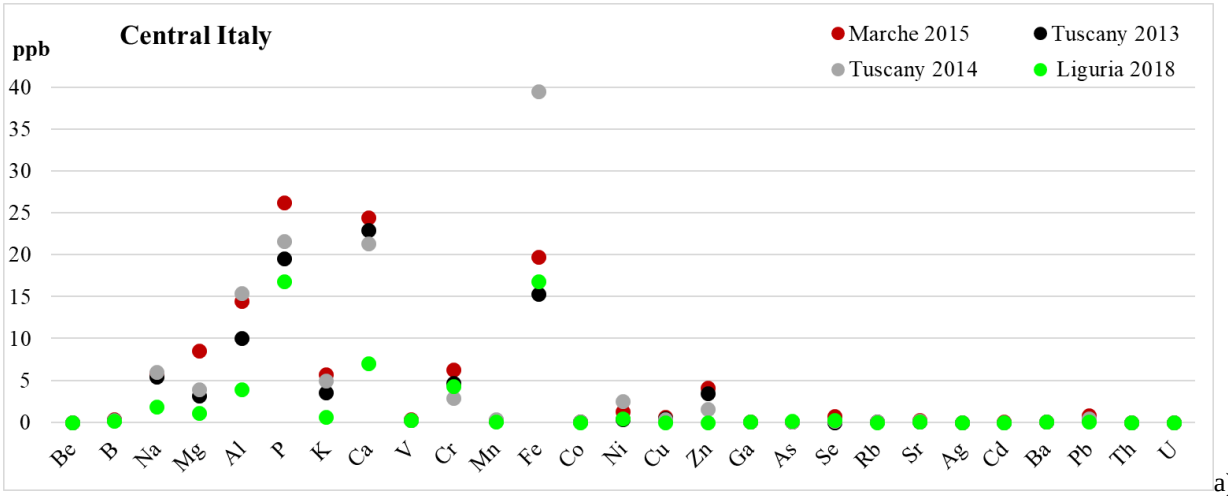
Central Italy
ppb
Marche 2015
Tuscany 2013
Tuscany 2014
Liguria 2018
40
35
30
25
20
15
10
5
0
Be B Na Mg Al P K Ca V Cr Mn Fe Co Ni Cu Zn Ga As Se Rb Sr Ag Cd Ba Pb Th U

a)

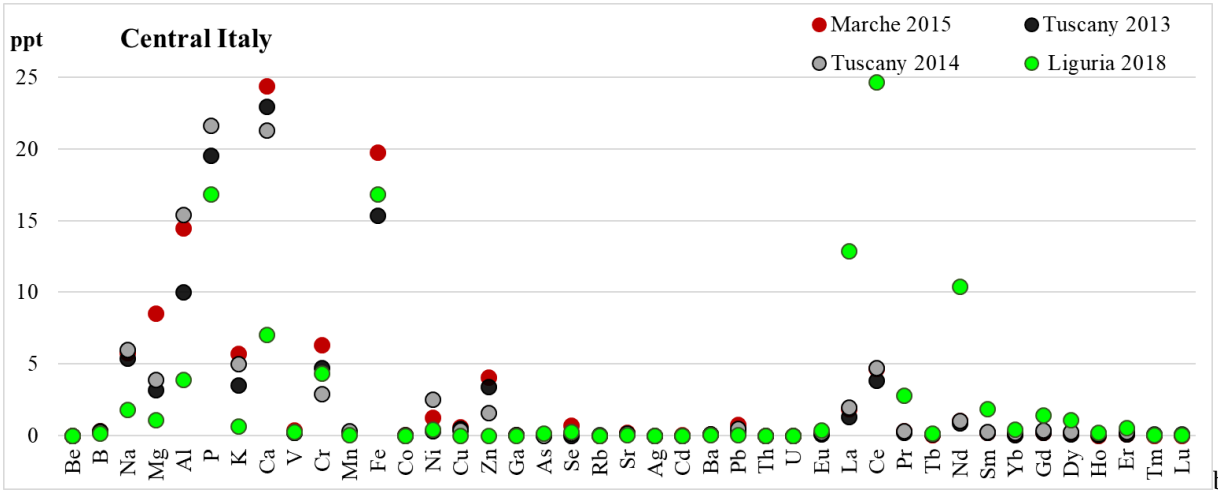
Central Italy
ppt
Marche 2015
Tuscany 2013
Tuscany 2014
Liguria 2018
25
20
15
10
5
0
Be B Na Mg Al P K Ca V Cr Mn Fe Co Ni Cu Zn Ga As Se Rb Sr Ag Cd Ba Pb Th U Eu La Ce Pr Tb Nd Sm Yb Gd Dy Ho Er Tm Lu

b)

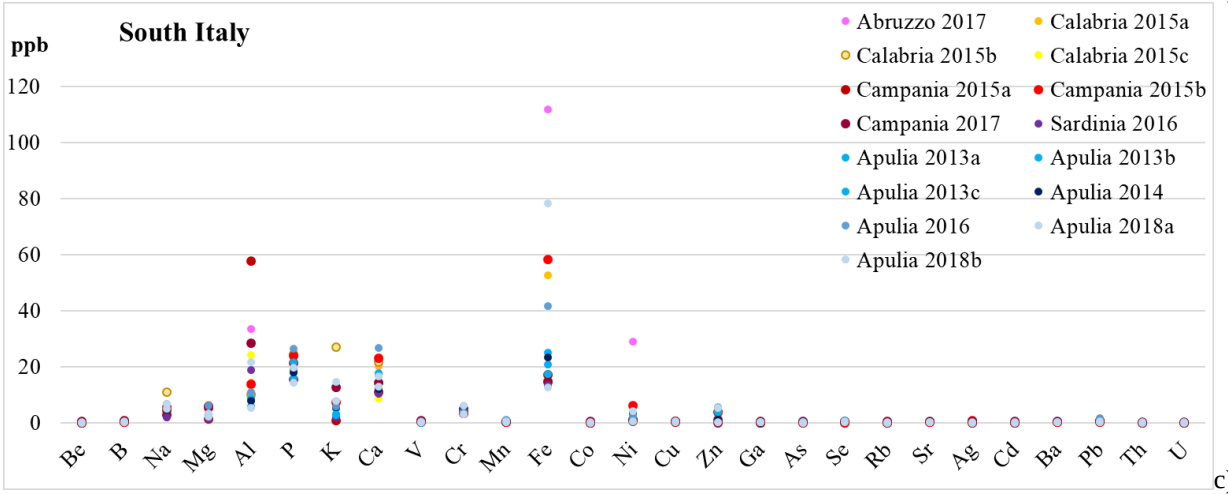
South Italy
ppb
Abruzzo 2017
Calabria 2015a
Calabria 2015b
Calabria 2015c
Campania 2015a
Campania 2015b
Campania 2017
Sardinia 2016
Apulia 2013a
Apulia 2013b
Apulia 2013c
Apulia 2014
Apulia 2016
Apulia 2018a
Apulia 2018b
120
100
80
60
40
20
0
Be B Na Mg Al P K Ca V Cr Mn Fe Co Ni Cu Zn Ga As Se Rb Sr Ag Cd Ba Pb Th U

c)

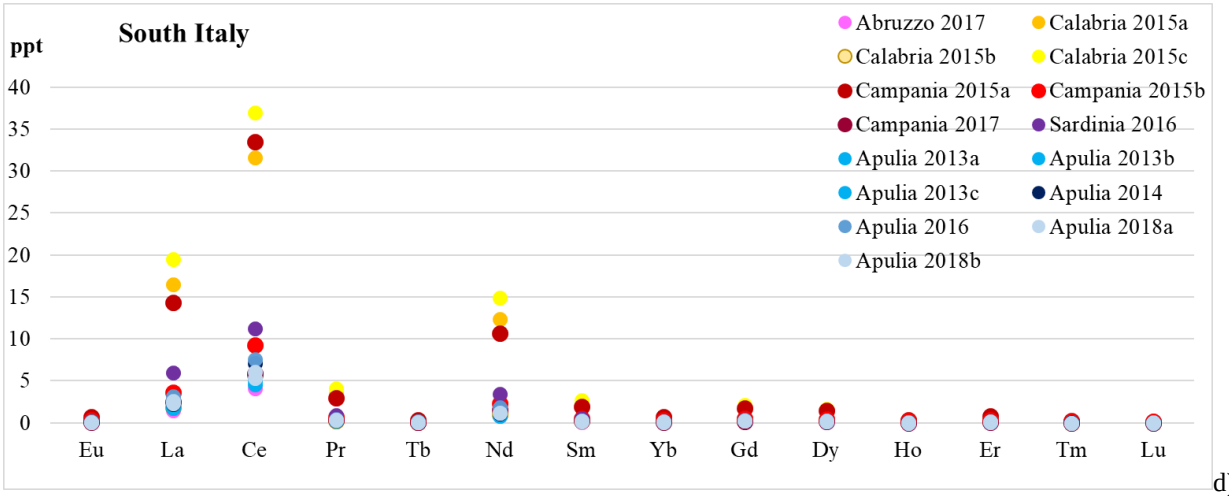
South Italy
ppt
Abruzzo 2017
Calabria 2015a
Calabria 2015b
Calabria 2015c
Campania 2015a
Campania 2015b
Campania 2017
Sardinia 2016
Apulia 2013a
Apulia 2013b
Apulia 2013c
Apulia 2014
Apulia 2016
Apulia 2018a
Apulia 2018b
40
35
30
25
20
15
10
5
0
Eu
La
Ce
Pr
Tb
Nd
Sm
Yb
Gd
Dy
Ho
Er
Tm
Lu

d)

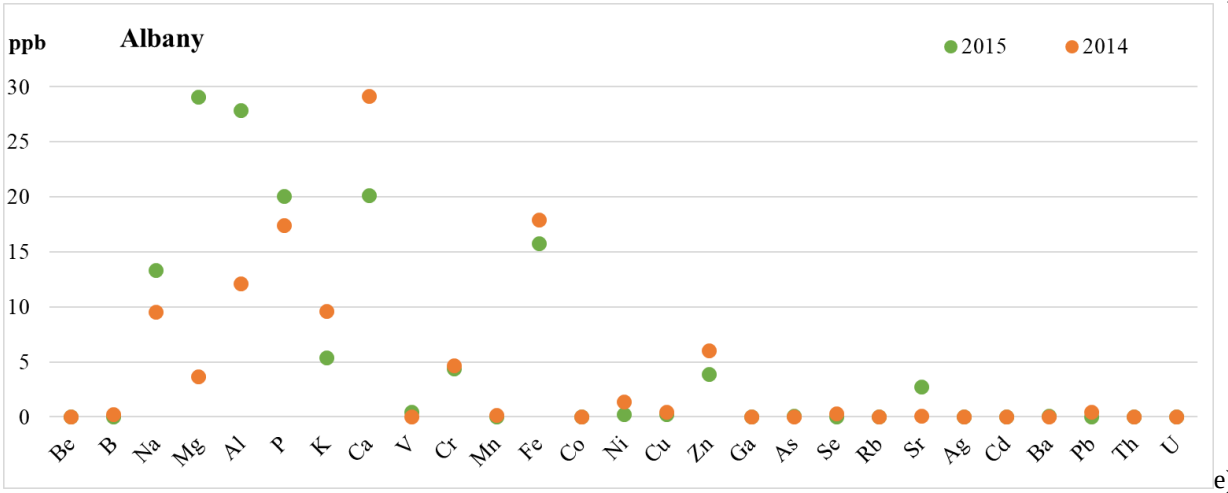
Albany
ppb
2015
2014
30
25
20
15
10
5
0
Be
B
Na
Mg
Al
P
K
Ca
V
Cr
Mn
Fe
Co
Ni
Cu
Zn
Ga
As
Se
Rb
Sr
Ag
Cd
Ba
Pb
Th
U

e)

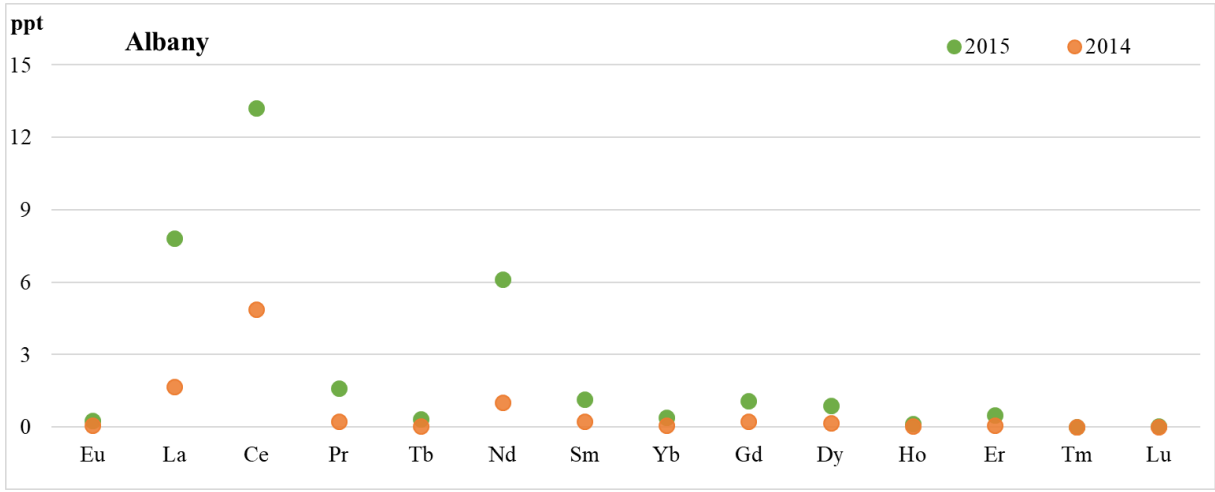
Albany
ppt
2015
2014
15
12
9
6
3
0
Eu
La
Ce
Pr
Tb
Nd
Sm
Yb
Gd
Dy
Ho
Er
Tm
Lu

f)

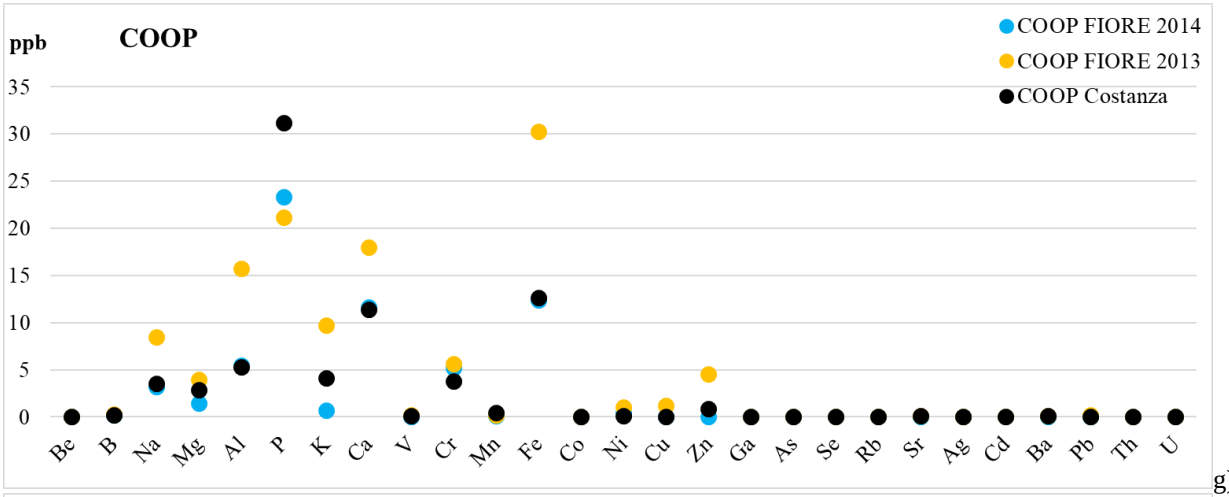
ppb
COOP
COOP FIORE 2014
COOP FIORE 2013
COOP Costanza
35
30
25
20
15
10
5
0
Be
B
Na
Mg
Al
P
K
Ca
V
Cr
Mn
Fe
Co
Ni
Cu
Zn
Ga
As
Se
Rb
Sr
Ag
Cd
Ba
Pb
Th
U

g)

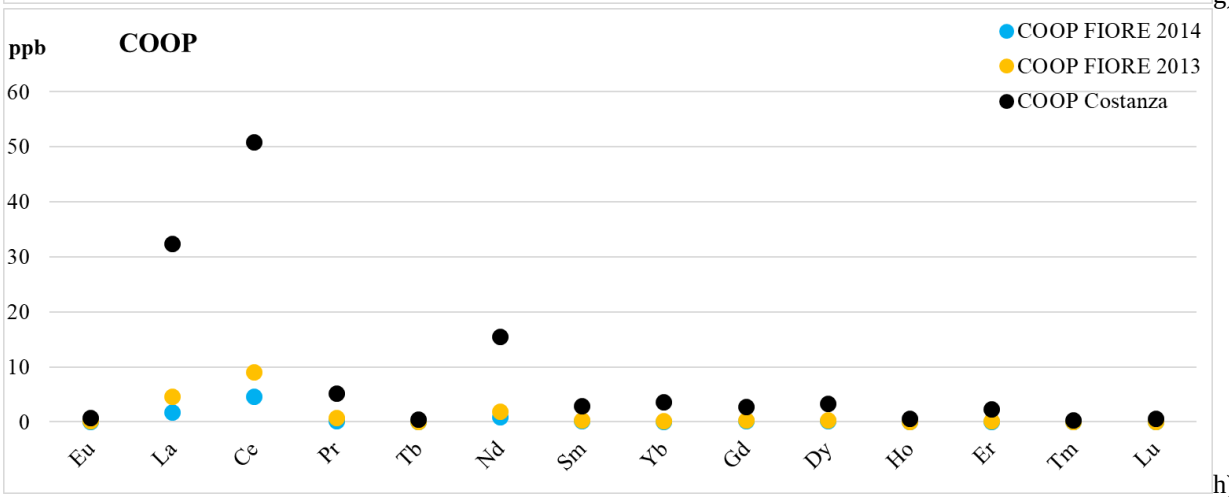
ppb
COOP
COOP FIORE 2014
COOP FIORE 2013
COOP Costanza
60
50
40
30
20
10
0
Eu
La
Ce
Pr
Tb
Nd
Sm
Yb
Gd
Dy
Ho
Er
Tm
Lu

h)

Figure 3

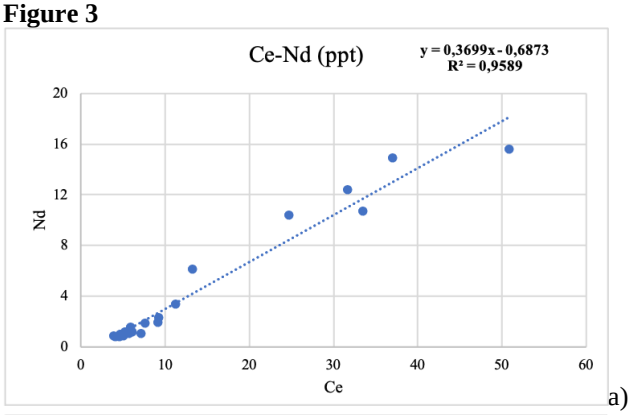

a)

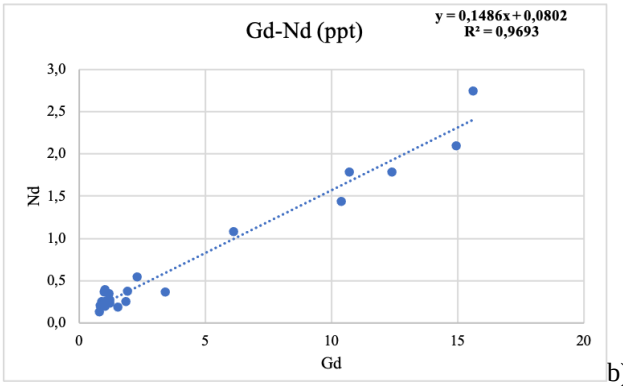

b)

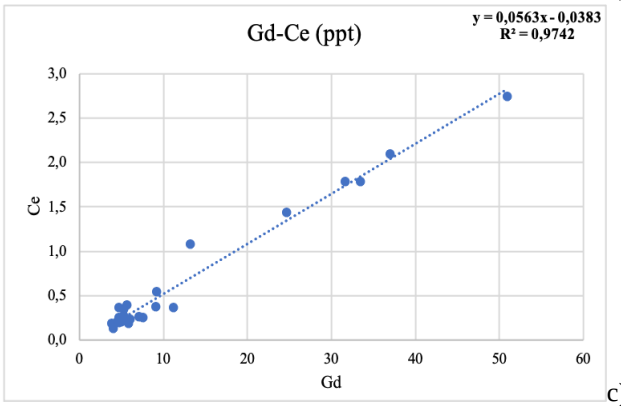

c)

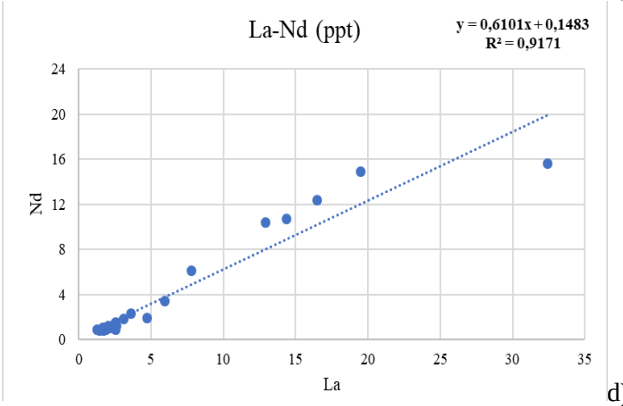

d)

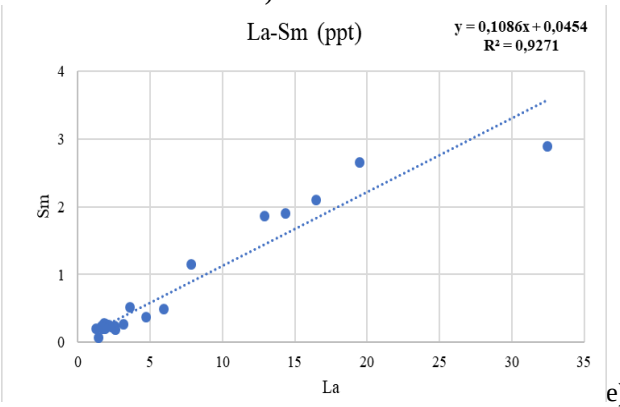

e)

Figure 4

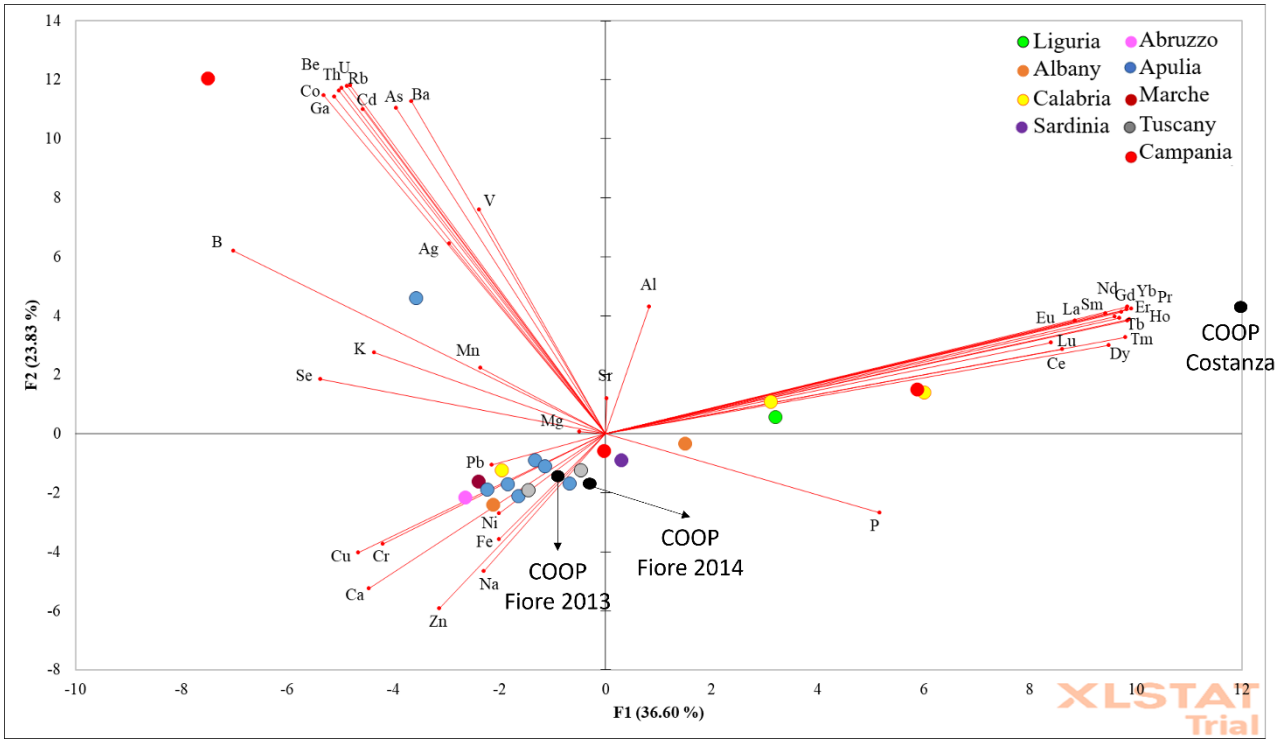
Liguria
Albany
Calabria
Sardinia
Abruzzo
Apulia
Marche
Tuscany
Campania
Be
Th
U
Rb
Co
Ga
Cd
As
Ba
V
B
Ag
Al
Nd
Gd
Yb
Pr
La
Sm
Er
Eu
Ho
Tb
Tm
Lu
Dy
Ce
K
Mn
Se
Sr
Mg
Pb
Ni
Fe
Cu
Cr
Ca
Na
Zn
P
COOP
Costanza
COOP
Fiore 2014
COOP
Fiore 2013
F2 (23.83 %)
F1 (36.60 %)
XLSTAT
Trial